Korean Journal of Radiology

KJR

Clinical Feasibility of Dual-Layer CT With Virtual Monochromatic Image for Preoperative Staging in Patients With Breast Cancer: A Comparison With Breast MRI

Bokdong Yeo[1], Kyung Min Shin[2], Byunggeon Park[2], Hye Jung Kim[2]*, Won Hwa Kim[2]*

[1]Department of Radiology, Kyungpook National University Hospital, Daegu, Republic of Korea
[2]Department of Radiology, School of Medicine, Kyungpook National University, Kyungpook National University Chilgok Hospital, Daegu, Republic of Korea

Objective: Dual-layer CT (DLCT) can create virtual monochromatic images (VMIs) at various monochromatic X-ray energies, particularly at low keV levels, with high contrast-to-noise ratio. The purpose of this study was to assess the clinical feasibility of contrast-enhanced chest DLCT with a low keV VMI for preoperative breast cancer staging, in comparison to breast MRI.
Materials and Methods: A total of 152 patients with 155 index breast cancers were enrolled in the study. VMIs were generated from contrast-enhanced chest DLCT at 40 keV and maximum intensity projection (MIP) with three-dimensional (3D) reconstruction was performed for both bilateral breast areas. Two radiologists reviewed in consensus the 3D MIP images of the chest DLCT with VMI and breast MRI in separate sessions with a 3-month wash-out period. The detection rate and mean tumor size of the index cancer were compared between the chest DLCT with VMI and breast MRI. Additionally, the agreement of tumor size measurement between the two imaging modalities were evaluated.
Results: Of all index cancers, 84.5% (131/155) were detected in the chest DLCT with VMI, while 88.4% (137/155) were detected in the breast MRI (P = 0.210). The Bland–Altman agreement between the chest DLCT with VMI and breast MRI was a mean difference of -0.05 cm with 95% limits of agreement of -1.29 to 1.19 cm. The tumor size in the chest DLCT with VMI (2.3 ± 1.7 cm) was not significantly different from that in the breast MRI (2.4 ± 1.6 cm) (P = 0.106).
Conclusion: The feasibility of chest DLCT with VMI was demonstrated for preoperative tumor staging in breast cancer patients, showing comparable cancer detectability and good agreement in tumor size measurement compared to breast MRI. This suggests that chest DLCT with VMI can serve as a potential alternative for patients who have contraindications to breast MRI.
Keywords: Breast cancer; Dual-layer CT; Virtual monochromatic image; Low keV; Cancer staging

INTRODUCTION

Recently, dual-energy CT (DECT) has emerged as an advanced clinical imaging technique that utilizes two different energy levels to acquire images. This method involves the simultaneous or sequential acquisition of CT data at two distinct X-ray energy levels, typically referred to as high and low energy levels. Dual-layer CT (DLCT) is a specific subtype of DECT, distinguished by its ability to automatically register the radiation spectrum received by two layers of a detector as two energetically different energy spectra, without altering the tube voltage and tube

current intensity used during the examination [1]. This unique feature allows all CT examinations performed with a dual layer detector to be retrospectively evaluated using the dual spectral technique, enabling the creation of virtual monochromatic images (VMIs) at various monochromatic X-ray energies.

When operating at low keV levels near the k-edge (33 keV) of iodine, there is a significant increase in contrast and enhanced visibility of lesions compared to traditional tube techniques including high keV levels. Despite the increased contrast, low-energy images exhibit high levels of noise. DLCT can overcome the noise by generating anti-correlated noise in photoelectric and Compton scatter images through simultaneous data collection from two different energy levels [2,3]. Early research and utilization of DLCT have been reported in various medical fields. Lennartz et al. [4] demonstrated that VMI obtained from head DLCT can improve the depiction of hypodense parenchymal lesions and intraparenchymal hemorrhage. Nagayama et al. [5] reported that abdomen DLCT with VMI improves image quality and detectability of hypovascular hepatic metastases compared to conventional CT. In the field of breast imaging, Inoue et al. [6] found that a high contrast-to-noise ratio (CNR) for breast carcinoma in VMIs of chest DLCT at an optimized energy level of 40 keV. Although conventional chest CT is limited for breast cancer staging due to low CNR, low keV VMIs of chest DLCTs could be utilized because of their high CNR.

To the best of our knowledge, no prior studies have investigated the feasibility of using chest DLCT with VMI for breast cancer staging. Therefore, the purpose of our study was to compare the cancer detection rate and breast tumor size measurement between a chest DLCT with VMI and breast MRI.

MATERIALS AND METHODS

Patients

We conducted a retrospective study that included 188 women diagnosed with primary breast cancer between September 2019 and August 2020. This retrospective study was approved by the Institutional Review Board of Kyungpook National University Chilgok Hospital (IRB No. 2023-11-022). These patients had not undergone neoadjuvant chemotherapy (NAC) and had undergone contrast-enhanced chest DLCT as part of their metastasis workup. Among these women, 29 patients did not undergo breast MRI and 7 patients underwent excisional

biopsy, resulting in the complete removal of the tumor. Consequently, a total of 152 patients who underwent chest DLCT and breast MRI were included in this study. The mean interval between chest DLCT and breast MRI was 14.9 days, with a standard deviation (SD) of 8.6 days and a range of 1–34 days. As three patients had bilateral breast cancers, a total of 155 index breast cancers were considered for the analysis.

Image Acquisition and Reconstruction

All chest DLCT data were acquired using 64-row spectral detector CT scanners (IQon®, Philips, Cleveland, OH, USA). The CT scan range extended from the lung base to the supraclavicular area, and it was acquired in the supine position. The routine clinical scanning parameters, without specific optimization, were as follows: slice collimation, 64 x 0.625 mm; pitch, 1.234; slice thickness, 1 mm; increment, 0.7 mm; rotation time, 0.27 seconds; and tube potential, 120 kVp. Dose modulation was enabled for all patients (DoseRight 3D-DOM, Philips). Intravenous administration of 1.2 mL/kg of a nonionic iodinated contrast medium (Iomeron 400®, Bracco, Milano, Italy) was performed at a flow rate of 2–2.5 mL/s, with a contrast bolus-delay of 40 seconds. The reconstructed field of view was individually adjusted using a 512 x 512 pixel-matrix. From the acquired raw data, images were reconstructed using a slice thickness of 1 mm and an increment of 0.7 mm with a hybrid iterative reconstruction algorithm (iDose4, level 3; Philips). The spectral image datasets, obtained through dual-layer detector technology that captured energy-dependent absorption information, allowed for the generation of VMIs using dedicated software (InteliSpace Portal version 10, Philips) in addition to the construction of conventionally processed CT images. Specifically, bilateral breast tissue of the chest was post-processed into three-dimensional maximum intensity projection (3D-MIP) images using the 40 keV VMI with the same software. The 3D-MIP reconstruction in this study included only the bilateral breast tissues and axillae, excluding the bilateral lung parenchyma, bony structures, and the heart within the chest CT region. The reconstructed 3D-MIP image allows rotation in all directions, enabling size measurements from the view that provides the largest visualization during interpretation. To assess radiation exposure, we examined the CT dose index volume (CTDIvol) and dose-length product (DLP) obtained from the DICOM data. Additionally, the effective dose was calculated. The estimated effective dose was calculated by

multiplying the DLP by a k-factor of 0.014 mSv·mGy^{-1}·cm^{-1} for the chest [7].

Breast MRI was performed with the patients in the prone position using a 3T system (Discovery MR750, GE Healthcare, Waukesha, WI, USA) equipped with a dedicated eight-channel surface breast coil. A total of 0.1 mL/kg of gadobutrol contrast agent (Gadovist, Bayer Schering Pharma, Berlin, Germany) was intravenously administered to each patient at a rate of 1 mL/s. Axial T1-weighted images (repetition time/echo time [TR/TE]: 746/10; matrix: 352 x 256; slice thickness: 3 mm) and axial fat-suppressed T2-weighted images (TR/TE: 8087/88; matrix: 384 x 256; slice thickness: 3 mm) were acquired. The dynamic contrast-enhanced bilateral axial MR examination included one precontrast phase and four or five postcontrast phases, utilizing three-dimensional gradient-echo, fat-suppressed, T1-weighted imaging (TR/TE: 4/2; matrix: 288 x 416; flip angle: 15°; slice thickness: 1 mm). Subtraction images and 3D-MIP images were generated for all studies.

Image Review

Reconstructed 3D-MIP images of the chest DLCT with VMI and breast MRI were reviewed on a dedicated workstation (PACS G3, Infinitt Healthcare Co., Seoul, South Korea). Tumorous lesions with greater enhancement compared to background parenchymal enhancement (BPE) were classified as cancerous. The analysis of the images involved measuring the longest diameter of the largest tumor in 3D reconstructed images of each modality (Fig. 1). As the reconstructed 3D-MIP images are rotatable, we identified the angle that maximized the tumor's longest diameter and conducted measurements accordingly. Two radiologists, with ten and two years of experience in breast imaging, respectively, performed cancer detection and size measurements in consensus. To minimize memory bias, they first reviewed the 3D-MIP images of the chest DLCT with VMI, and after a three-month wash-out period, reviewed the 3D-MIP images of the breast MRI. The radiologists were blinded to any clinical information, histopathological diagnosis, and additional imaging data.

Statistical Analysis

The pathological size of the breast cancer used in this study includes the in situ component. In cases where multiple lesions were present, the largest diameter of the largest tumor in the breast was used for comparison. The size discrepancy was calculated by subtracting the tumor
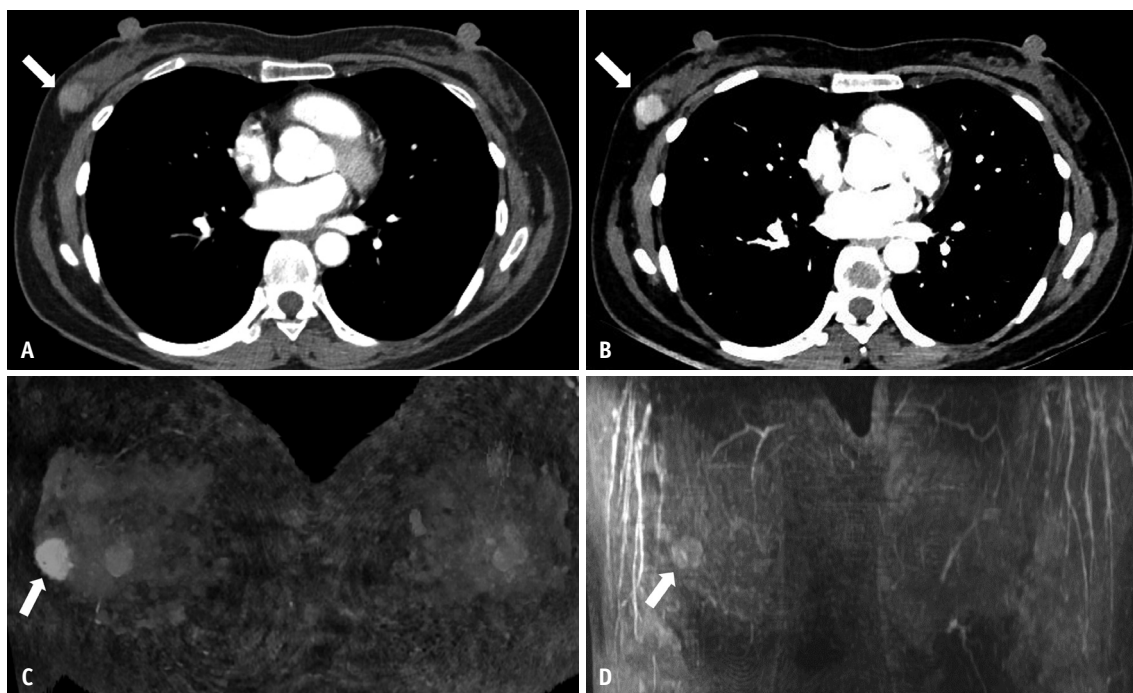
Fig. 1. A 47-year-old woman with invasive ductal carcinoma in the right breast. **A, B:** An axial image of the conventional contrast-enhanced chest CT and VMI of the contrast-enhanced chest DLCT at 40 keV, depicting the level of right breast cancer (arrows). **C:** Reconstructed 3D MIP of the VMI of the chest DLCT. The longest diameter of the tumor (arrow) was measured as 2.1 cm. **D:** 3D MIP image of the breast MRI. The longest diameter of the tumor (arrow) was measured as 1.9 cm. Pathological tumor size was 2.0 cm. VMI = virtual monochromatic image, DLCT = dual-layer CT, 3D = three-dimensional, MIP = maximum intensity projection

size measured by each modality from that determined by pathological examination. The McNemar test was used to compare the detectability of the chest DLCT with VMI and breast MRI. The agreement in tumor size measurement between the chest DLCT and breast MRI was analyzed using Bland–Altman plots. We also employed a paired *t*-test to assess the significance of the difference between the mean tumor sizes measured by chest DLCT and breast MRI. Furthermore, the agreement among the chest DLCT, breast MRI, and pathology regarding tumor size was evaluated using the intraclass correlation coefficient (ICC), employing a two-way mixed model with an absolute agreement definition and a single measure. The degree of ICC reliability was based on a widely cited reference in the field [8]. Concordance between the tumor sizes obtained from each modality and the pathological size was defined arbitrarily as a difference within ±5 mm. Underestimation was defined as a difference less than -5 mm, and overestimation was defined as a difference greater than 5 mm. The chi-square test was used to compare the concordance between the two modalities. All statistical analyses were performed using MedCalc software (version 20.114, MedCalc, Ostend, Belgium). A *P*-value less than 0.05 was considered statistically significant.

RESULTS

Patient and Tumor Characteristics

Table 1 summarizes the characteristics of 152 patients with a total of 155 index cancers. The mean age of the patients was 51.5 years, with a range of 26–72 years. Out of the 155 index breast cancers, 121 (78.0%) were invasive ductal carcinoma (IDC), 14 (9.0%) were invasive lobular carcinoma, and 10 (6.5%) were ductal carcinoma in situ. The remaining 10 (6.5%) breast cancers consisted of the following subtypes: four mucinous carcinomas, three microinvasive ductal carcinomas, one metaplastic carcinoma, one microinvasive papillary carcinoma, and one mixed invasive ductal and lobular carcinoma. The mean pathological size of the invasive component of the tumors was 1.6 cm, with a SD of 0.9 cm and a range of 0–6.0 cm. The mean of the total pathological tumor size, including the in situ component, was 2.2 cm, with a SD of 1.3 cm and a range of 0.7–8.5 cm.

Cancer Detection: Chest DLCT With VMI vs. Breast MRI

Among the 155 index cancers included in the study, 131 (84.5%) were detected in the chest DLCT with VMI and 137

Table 1. Patient and tumor characteristics

Characteristics	Value
Patient (n = 152)	
Age, yrs	51.5 ± 8.5
Tumor (n = 155)	
Size (all), cm	2.2 ± 1.3
Size (invasive), cm	1.6 ± 0.9
Subtype	
IDC	121 (78.0)
ILC	14 (9.0)
DCIS	10 (6.5)
Others*	10 (6.5)
T stage	
T1	92 (59.4)
T2	58 (37.4)
T3	5 (3.2)
Menopausal status	
Pre	81 (52.3)
Post	74 (47.7)
Amount of fibroglandular tissue on MRI	
Almost entirely fat	0 (0)
Scattered fibroglandular tissue	12 (7.7)
Heterogeneous fibroglandular tissue	126 (81.3)
Extreme fibroglandular tissue	17 (11.0)
BPE	
Minimal	83 (53.5)
Mild	35 (22.6)
Moderate	30 (19.4)
Marked	7 (4.5)
ER status	
Positive	128 (82.6)
Negative	27 (17.4)
PR status	
Positive	117 (75.5)
Negative	38 (24.5)
HER2 status	
Positive	25 (16.1)
Negative	130 (83.9)
Detection method	
Screening	75 (48.4)
Diagnostic	80 (51.6)
Histologic grade	
1	9 (5.8)
2	89 (57.4)
3	57 (36.8)
Surgery	
Mastectomy	34 (21.9)
BCS	121 (78.1)

Data are numbers of tumors, with percentages in parentheses, except for patient age and tumor size which are presented in mean ± standard deviation.
*Others include mucinous (4), microinvasive ductal (3), metaplastic (1), microinvasive papillary (1) and mixed invasive ductal and lobular (1) carcinomas.
IDC = invasive ductal carcinoma, ILC = invasive lobular carcinoma, DCIS = ductal carcinoma in situ, BPE = background parenchymal enhancement, ER = estrogen receptor, PR = progesterone receptor, HER2 = human epidermal growth factor receptor 2, BCS = breast conserving surgery

(88.4%) were found in the breast MRI (P = 0.210) (Table 2). This indicates that there was no significant difference in the cancer detection rates between the chest DLCT with VMI and breast MRI. Among the 155 index cancers, 126 lesions were detected in both chest DLCT with VMI and breast MRI, 5 lesions were exclusively identified in the chest DLCT with VMI, and 11 lesions were exclusively identified in the breast MRI. All three bilateral breast cancers (total 6 breast cancer lesions) were detected in both chest DLCT with VMI and breast MRI (Fig. 2). Thirteen index cancers were not detected by either chest DLCT with VMI or breast MRI. The mean pathological size of these 13 cancers was 1.7 cm, with an SD of 1.0 cm and a range of 0.7–4.0 cm. Among these 13 cancers, 8 were IDC, 3 were ILC, and the remaining were microinvasive carcinoma. In terms of the amount of fibroglandular tissue on breast MRI, all breast parenchyma exhibited high grade (11 were classified as category c, and 2 as category d). Regarding the BPE of the breast MRI, more than half of the breasts had higher-level enhancement (5 were moderate and 3 were marked). Among the 5 cancers with lower-level (minimal or mild) BPE, all except one were smaller than 1 cm. Most of these cancers were identified as masses on breast ultrasonography or microcalcifications on mammography. The information regarding the 13 undetected cancers is summarized in Table 3.
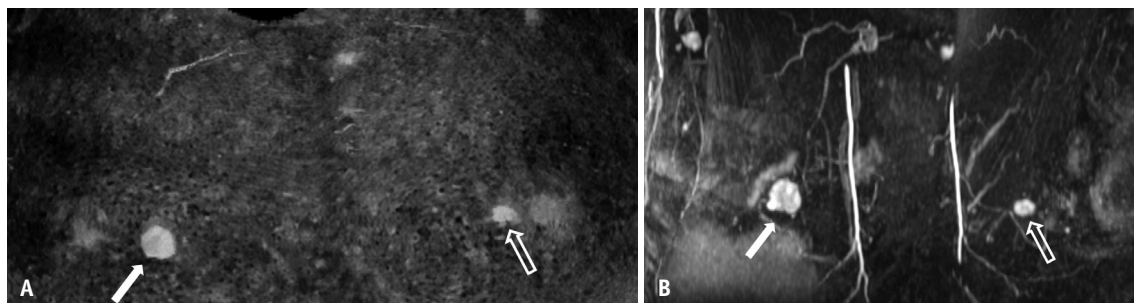
Tumor Measurement

The agreement between the chest DLCT with VMI and breast MRI is presented as a Bland–Altman plot in Figure 3, with the mean difference of -0.05 cm and 95% limits of agreement of -1.29 to 1.19 cm. There was no significant difference in the tumor size between the chest DLCT with VMI and breast MRI, with the chest DLCT with VMI measuring a mean size of 2.3 cm (SD = 1.7 cm, range: 0.7–9.7 cm) and breast MRI measuring a mean size of 2.4 cm (SD = 1.6 cm, range: 0.6–8.4 cm) (P = 0.106). The ICC for the chest DLCT with VMI compared to the breast MRI was 0.840 (P < 0.001), indicating good agreement. The additional explanation of correlation and agreement among the chest DLCT with VMI, breast MRI, and pathology are provided in Supplementary Materials, Supplementary Table 1, and Supplementary Figure 1.

The concordances between each modality and pathology are as follows. Among the 131 lesions detected in the chest DLCT with VMI, 87 lesions (66.4%) were concordantly measured, 25 lesions (19.1%) were overestimated, and 19 lesions (14.5%) were underestimated. Among the 137 lesions detected in breast MRI, 97 lesions (70.8%) were concordantly measured, 24 lesions (17.5%) were overestimated, and 16 lesions (11.7%) were underestimated. Breast MRI exhibited a slightly higher rate of concordance compared with chest DLCT with VMI (P = 0.440) without statistical significance.

Radiation Dose

The mean CTDIvol, DLP, and effective dose values were 5.07 ± 1.06 mGy, 247.1 ± 50.3 mGy·cm, and 3.46 ± 0.70 mSv, respectively.

Table 2. Cancer detection rate of chest DLCT with virtual monochromatic image and breast MRI

	MRI-detected	MRI-not detected	Total
DLCT-detected	126 (81.3)	5 (3.2)	131 (84.5)
DLCT-not detected	11 (7.1)	13 (8.4)	24 (15.5)
Total	137 (88.4)	18 (11.6)	155 (100)

Data are numbers of cancers, with percentages in parentheses.
DLCT = dual-layer CT

Fig. 2. A 60-year-old woman with bilateral invasive ductal carcinoma. **A:** In the reconstructed 3D MIP of the virtual monochromatic image of the chest dual-layer CT, the longest diameter of the right tumor (arrow) was measured as 2.0 cm, and that of the left tumor (empty arrow) was measured as 1.3 cm. **B:** In the 3D MIP image of the breast MRI, the longest diameter of the right tumor (arrow) was measured as 1.7 cm, and that of the left tumor (empty arrow) was measured as 1.1 cm. The pathological tumor sizes were 2.0 cm and 1.3 cm, respectively. 3D = three-dimensional, MIP = maximum intensity projection

Table 3. Pathologic and radiologic information of 13 cancers not detected by either method and background breast parenchyma

Cancer	Pathologic size, invasive (cm)	Pathologic size, total (cm)	Histology	FGT of MRI	BPE of MRI	Imaging findings on MMG	Imaging findings on USG
1	0.7	1.7	IDC	c	Moderate	Negative	Mass
2	1.3	1.3	IDC	c	Moderate	Architectural distortion	Mass
3	0.2	1.3	IDC	c	Marked	Mcs	Mcs
4	0.9	0.9	IDC	c	Minimal	Mass with architectural distortion	Mass
5	0	2.5	Microinvasive papillary carcinoma	c	Marked	Asymmetry	Non-mass lesion
6	2.8	2.8	ILC	d	Moderate	Negative	Mass
7	0.7	0.7	IDC	c	Mild	Negative	Mass
8	0.7	0.7	ILC	c	Mild	Negative	Mass
9	0.1	4.0	Microinvasive ductal carcinoma	c	Marked	Mcs	Non-mass lesion with Mcs
10	2.8	2.8	ILC	d	Moderate	Negative	Mass
11	1.1	1.1	IDC	c	Moderate	Negative	Mass
12	0.7	0.7	IDC	c	Minimal	Negative	Mass
13	0.4	1.2	IDC	c	Mild	Mcs	Non-mass lesion with Mcs

Amount of FGT of breast MRI are explained by alphabet of BI-RADS grades (c, heterogeneous FGT; d, extreme FGT).
FGT = fibroglandular tissue, BI-RADS = Breast Imaging Reporting and Data System, BPE = background parenchymal enhancement, MMG = mammography, USG = ultrasonography, IDC = invasive ductal carcinoma, Mcs = microcalcifications, ILC = invasive lobular carcinoma
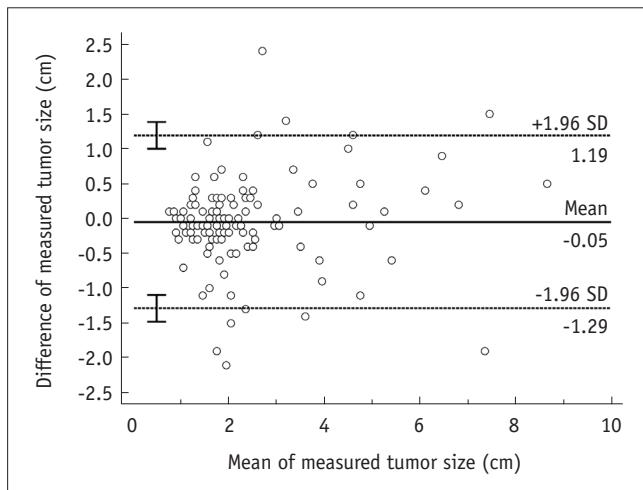
Fig. 3. Bland–Altman plot between the chest DLCT with VMI and breast MRI. The solid line indicates the mean difference (-0.05 cm) between the measured tumor size in the chest DLCT with VMI and that in the breast MRI. The dotted lines represent the upper and lower limits of agreement, indicating the range within which 95% of the differences between the two measurements lie (-1.29 cm and 1.19 cm, respectively). DLCT = dual-layer CT, VMI = virtual monochromatic image, SD = standard deviation

DISCUSSION

In breast cancer staging, the American College of

Radiology offers guidelines on the use of breast MRI and chest CT [9]. Breast MRI has been considered the most accurate imaging tool for providing anatomical information with a high spatial resolution, and is widely used for breast cancer staging. Chest CT is usually used in the assessment of distant metastasis for the evaluation of recurrent or stage IV breast cancer cases [10]. It is not primarily used in the assessment in-breast lesions, despite a report that the positive predictive value for malignancy of incidentally found breast nodules is as substantial as 28.4% [11].

There have only been a few reports regarding CT examination of breast cancer. In 2016, Okamura et al. [12] analyzed 43 breast cancer patients using dual-source DECT and found that the CT density of tumors was higher than that of normal breast tissue, indicating the potential utility of DECT in evaluating breast cancer. In 2020, Volterrani et al. [13] reported on the use of low keV monochromatic images for staging 67 locoregional breast cancers. They found that the T category was correctly identified in 85.2% of the cases compared to pathology, with no statistically significant difference. In this study, we demonstrated the potential of MIP images of low-keV VMIs obtained from chest DLCT in the detection and size measurement of breast cancer. There was no significant difference in cancer detectability between

the chest DLCT with VMI and breast MRI. Furthermore, the measured tumor sizes obtained using the chest DLCT with VMI demonstrated a good agreement (ICC: 0.840, P < 0.001) with those obtained using the breast MRI. Additionally, it showed favorable concordance (66.4%, with a 5 mm limit) with pathological results. Therefore, we believe that chest DLCT with VMI could serve as a reliable complement to MRI in inevitable cases, such as in patients with claustrophobia or limited access to MRI facilities. Despite being considered the most effective modality, breast MRI requires a substantial amount of time, with a minimum duration of 30–40 minutes per examination. On the contrary, CT is a crucial imaging technique that offers short scan times and is essential for assessing the extent of the overall lesion, as well as identifying metastasis and concurrent pulmonary conditions. However, when using CT instead of MRI, one should consider factors such as radiation exposure and potential side effects from CT contrast agents, and carefully weigh the individual risk–benefit ratio. In this study population, the mean effective dose was 3.46 ± 0.70 mSv. For comparison, the typical effective dose per scan is 0.36 mSv for mammography and 6.2 mSv for chest CT, respectively [14].

Even though there was no significant difference, it is essential to consider the factors associated with tumor detectability and size measurement in the chest DLCT with VMI and breast MRI. Considering the characteristics of undetected cancers in Table 3, it appears that the detection of cancer was less successful in cases with sub-centimeter tumor size or higher BPE. In terms of size measurement, differences in the patients' positioning and image acquisition timing after contrast injection in the breast MRI and chest DLCT need to be considered. Breast MRI is conducted with the patient in a prone position, facilitating the visualization of breast parenchyma, including the lesion, in an extended state due to gravitational effects. In contrast, CT imaging is performed with the patient in a supine position, which compresses the breast tissue. Additionally, the chest DLCTs were acquired 40 seconds after intravenous contrast injection, whereas the first phase of the dynamic enhancement sequence in the breast MRIs was acquired within 120 seconds after the injection. This temporal difference may also account for variations in the detectability and size measurement of specific lesions between modalities.

There are several limitations of our study. Firstly, this study lacks consideration of the detection and evaluation of multifocal/multicentric malignant lesions and the relation

between the primary lesion and surrounding structure, which is one of the primary purposes of breast MRI. Therefore, there is a limitation in staging and evaluating the extent of breast cancer when using the chest DLCT. Second, the detectability and measured tumor sizes were acquired through consensus, which is discouraged in radiology research and poses limitations. Additionally, tumor size was measured exclusively on MIP images and not on other MRI sequences or CT images. However, Choi et al. [15] reported that MIP images are the most accurate for measuring tumor size in breast MRI, particularly when the tumor size is below 2 cm. Third, the quality of image reconstruction could have potentially influenced the results of this study. We acknowledge that the reconstruction process was carried out by a single technician who possessed extensive experience of over 10 years in our hospital. While this technician's expertise is valuable, it is important to consider that the clarity and accuracy of the reconstructed images might be influenced by various factors, including the inclusion of specific anatomical structures. To ensure consistency, standardized reconstruction methods, such as MIP images used in MRI, may be necessary. Fourth, comparing CT, performed in the supine position, with MRI, performed in the prone position, presents challenges in accurate comparisons. To overcome this limitation, our institution is planning to conduct a study with a prone positioning protocol for DLCT similar to the one used for breast MRI. Subsequent studies using this device are planned to address this issue and improve comparability. Lastly, this study focused on patients who did not require NAC according to the hospital protocol. It is known that concordance between imaging modalities and pathology can decrease when breast cancer is treated with NAC [16]. Thus, accuracy may differ when comparing to the gold standard of pathology for patients with higher stages of breast cancer undergoing NAC. However, it is generally expected that enhancement levels increase with larger lesions, potentially leading to higher detection rates. Additionally, applications such as lymph node metastasis or other additional lesion evaluation are believed to be possible, and further research in these areas is needed to fully explore their potential.

In conclusion, we demonstrated the feasibility of using chest DLCT with VMI for assessing breast cancer extent for preoperative tumor staging, showing comparable cancer detectability and good agreement in tumor size measurement compared to breast MRI. The use of low keV VMI with high CNR in chest DLCT can be a potential

alternative for breast cancer staging in patients with contraindications to breast MRI.

Supplement

The Supplement is available with this article at https://doi.org/10.3348/kjr.2023.1312.

Availability of Data and Material

The datasets generated or analyzed during the study are available from the corresponding author on reasonable request.

Conflicts of Interest

The authors have no potential conflicts of interest to disclose.

Author Contributions

Conceptualization: Won Hwa Kim. Data curation: Bokdong Yeo. Formal analysis: Bokdong Yeo. Investigation: Byunggeon Park. Methodology: Hye Jung Kim. Project administration: Won Hwa Kim. Resources: Kyung Min Shin. Software: Won Hwa Kim. Supervision: Hye Jung Kim. Validation: Won Hwa Kim. Visualization: Byunggeon Park. Writing—original draft: Bokdong Yeo. Writing—review & editing: Kyung Min Shin, Hye Jung Kim.

ORCID IDs

Bokdong Yeo
   https://orcid.org/0009-0005-8211-3918
Kyung Min Shin
   https://orcid.org/0000-0003-4109-0228
Byunggeon Park
   https://orcid.org/0000-0002-5807-9271
Hye Jung Kim
   https://orcid.org/0000-0002-0263-0941
Won Hwa Kim
   https://orcid.org/0000-0001-7137-9968

REFERENCES

1. Goo HW, Goo JM. Dual-energy CT: new horizon in medical imaging. *Korean J Radiol* 2017;18:555-569
2. Rassouli N, Etesami M, Dhanantwari A, Rajiah P. Detector-based spectral CT with a novel dual-layer technology: principles and applications. *Insights Imaging* 2017;8:589-598
3. Nagayama Y, Nakaura T, Oda S, Utsunomiya D, Funama Y, Iyama Y, et al. Dual-layer DECT for multiphasic hepatic CT with 50 percent iodine load: a matched-pair comparison with a 120 kVp protocol. *Eur Radiol* 2018;28:1719-1730
4. Lennartz S, Laukamp KR, Neuhaus V, Große Hokamp N, Le Blanc M, Maus V, et al. Dual-layer detector CT of the head: initial experience in visualization of intracranial hemorrhage and hypodense brain lesions using virtual monoenergetic images. *Eur J Radiol* 2018;108:177-183
5. Nagayama Y, Iyama A, Oda S, Taguchi N, Nakaura T, Utsunomiya D, et al. Dual-layer dual-energy computed tomography for the assessment of hypovascular hepatic metastases: impact of closing k-edge on image quality and lesion detectability. *Eur Radiol* 2019;29:2837-2847
6. Inoue T, Nakaura T, Iyama A, Kidoh M, Nagayama Y, Uetani H, et al. Usefulness of virtual monochromatic dual-layer computed tomographic imaging for breast carcinoma. *J Comput Assist Tomogr* 2020;44:78-82
7. Trattner S, Halliburton S, Thompson CM, Xu Y, Chelliah A, Jambawalikar SR, et al. Cardiac-specific conversion factors to estimate radiation effective dose from dose-length product in computed tomography. *JACC Cardiovasc Imaging* 2018;11:64-74
8. Koo TK, Li MY. A guideline of selecting and reporting intraclass correlation coefficients for reliability research. *J Chiropr Med* 2016;15:155-163
9. American College of Radiology. ACR appropriateness criteria®: imaging of invasive breast cancer [accessed on October 24, 2023]. Available at: https://acsearch.acr.org/docs/3186697/narrative
10. Gradishar WJ, Moran MS, Abraham J, Aft R, Agnese D, Allison KH, et al. Breast cancer, version 3.2022, NCCN clinical practice guidelines in oncology. *J Natl Compr Canc Netw* 2022;20:691-722
11. Moyle P, Sonoda L, Britton P, Sinnatamby R. Incidental breast lesions detected on CT: what is their significance? *Br J Radiol* 2010;83:233-240
12. Okamura Y, Yoshizawa N, Yamaguchi M, Kashiwakura I. Application of dual-energy computed tomography for breast cancer diagnosis. *Int J Med Phys Clin Eng Radiat Oncol* 2016;5:288-297
13. Volterrani L, Gentili F, Fausto A, Pelini V, Megha T, Sardanelli F, et al. Dual-energy CT for locoregional staging of breast cancer: preliminary results. *AJR Am J Roentgenol* 2020;214:707-714
14. Mettler FA Jr, Mahesh M, Bhargavan-Chatfield M, Chambers CE, Elee JG, Frush DP, et al. Patient exposure from radiologic and nuclear medicine procedures in the United States: procedure volume and effective dose for the period 2006-2016. *Radiology* 2020;295:418-427
15. Choi WJ, Cha JH, Kim HH, Shin HJ, Chae EY. The accuracy of breast MR imaging for measuring the size of a breast cancer:

analysis of the histopathologic factors. *Clin Breast Cancer* 2016;16:e145-e152

16. Ramirez SI, Scholle M, Buckmaster J, Paley RH, Kowdley GC. Breast cancer tumor size assessment with mammography, ultrasonography, and magnetic resonance imaging at a community based multidisciplinary breast center. *Am Surg* 2012;78:440-446